ISSN 1674-1056
http://cpb.iphy.ac.cn
http://iopscience.iop.org/cpb
中国物理 B
Chinese Physics
中国物理 Chinese Physics B

Dynamics of the Au+H_2 reaction by time-dependent wave packet and quasi-classical trajectory methods

Yong Zhang(张勇), Chengguo Jiang(姜成果)
Citation: Chin. Phys. B . 2019, 28(12): 123101 . **doi:** 10.1088/1674-1056/ab52f2
Journal homepage: http://cpb.iphy.ac.cn; http://iopscience.iop.org/cpb

What follows is a list of articles you may be interested in

Reaction mechanism of D+ND→N+D_2 and its state-to-state quantum dynamics

Ting Xu(许婷), Juan Zhao(赵娟), Xian-Long Wang(王宪龙), Qing-Tian Meng(孟庆田)
Chin. Phys. B . 2019, 28(2): 023102 . **doi:** 10.1088/1674-1056/28/2/023102

State-to-state dynamics of F(^{2}P)+HO($^2\Pi$) →O(^{3}P)+HF($^1\Sigma^+$) reaction on 1^3A" potential energy surface

Juan Zhao(赵娟), Hui Wu(吴慧), Hai-Bo Sun(孙海波), Li-Fei Wang(王立飞)
Chin. Phys. B . 2018, 27(2): 023102 . **doi:** 10.1088/1674-1056/27/2/023102

State-to-state quantum dynamics of N(^{2}D)+HD (v=0, j=0) reaction

Yong Zhang(张勇)
Chin. Phys. B . 2016, 25(12): 123104 . **doi:** 10.1088/1674-1056/25/12/123104

State-to-state quantum dynamics of the N(^{4}S)+H_2 ($X^1\Sigma^+$)→NH($X^3\Sigma^-$)+H(^{2}S) reaction and its reaction mechanism analysis

Zhang Jing, Gao Shou-Bao, Wu Hui, Meng Qing-Tian
Chin. Phys. B . 2015, 24(8): 083104 . **doi:** 10.1088/1674-1056/24/8/083104

Translational, vibrational, rotational enhancements and alignments of reactions H+ClF (v=0–5, j=0, 3, 6, 9) →HCl+F and HF+Cl,at E_{rel}=0.5–20 kcal/mol

Victor Wei-Keh Chao(Wu)
Chin. Phys. B . 2013, 22(10): 103101 . **doi:** 10.1088/1674-1056/22/10/103101

Dynamics of the Au + H_2 reaction by time-dependent wave packet and quasi-classical trajectory methods

Yong Zhang(张勇)† and Chengguo Jiang(姜成果)

Department of Physics, Tonghua Normal University, Tonghua 134002, *China*

(Received 30 August 2019; revised manuscript received 15 October 2019; published online 29 November 2019)

Dynamics of the Au + H_2 reaction are studied using time-dependent wave packet (TDWP) and quasi-classical trajectory (QCT) methods based on a new potential energy surface [*Int. J. Quantum Chem.* **118** e25493 (2018)]. The dynamic properties such as reaction probability, integral cross section, differential cross section and the distribution of product are studied at state-to-state level of theory. Furthermore, the present results are compared with the theoretical studies available. The results indicate that the complex-forming reaction mechanism is dominated in the reaction in the low collision energy region and the abstract reaction mechanism plays a dominant role at high collision energies. Different from previous theoretical calculations, the side-ways scattering signals are found in the present work and become more and more apparent with increasing collision energy.

Keywords: reaction probability, integral cross section, time-dependent wave packet, quasi-classical trajectory

PACS: 31.15.xv, 34.50.–s, 03.67.Lx **DOI:** 10.1088/1674-1056/ab52f2

1. Introduction

Since the excellent catalytic effect of gold nano-cluster on low temperature oxidation reaction of CO was found by Haruta and co-workers[1] in 1989, a number of experiments have been performed on nanoscale gold clusters. In addition, properties of nanoscale gold clusters such as electronic, optical, chemical, and catalytic were reported in previous theoretical studies.[2–9] To further explore the properties of gold and its clusters, a lot of theoretical studies have been carried out for the reaction of transition metallic element Au and its ions with H_2 molecules.[10–20] Using the complete active space self-consistent field (CASSCF) and configuration interaction method, two low-lying electronic states of AuH_2 systems were studied by Balasubramania and Liao[10] in 1988. The group of Balasubramanian[11] restudied the AuH_2 system in 2004. In their work, the bending potential energy surface (PES) was studied using the CASSCF/MRSDCI methods on three low-lying electronic states of AuH_2 systems and they found that there is a barrier on the path when the ground state AuH_2 system decompose into Au(^2S) + H_2 channel. Using highly correlated wave functions with atomic pseudopotentials and spin–orbit interactions, the electronic structure, reactivity, and spectroscopy of the AuH_2 system were investigated by Chambaud *et al.*[12] in 2005.

As far as we know, there are few studies on dynamics of the Au + H_2 reaction due to no global PES of AuH_2 systems until 2010. The first global PES of the ground state of AuH_2 system was constructed by Zanchet *et al.*, called the Zanchet PES.[13] In the *ab initio* calculation, multi-reference configuration interaction (MRCI) method with one-electron Gaussian-type basis set ECP60MDF[21] and augmented correlation-consistent polarization valence triple zeta (AVTZ)[22] basis set were employed. Then, the PES was constructed through GFIT3 C procedure[23–25] by fitting 2376 *ab initio* points. Based on the Zanchet PES, some dynamics studies have been performed. For example, the reactions of Au with H_2 and its isotopic variant HD, D_2 were studied by Yuan and co-workers[14,15] using the time-dependent wave packet (TDWP) and quasi-classical trajectory (QCT) methods. The dynamic properties such as reaction probability, integral cross section (ICS), and differential cross section (DCS) were studied at state-to-state level of theory. The Zanchet PES with relative little *ab initio* points and the basis sets used in the *ab initio* calculation also have a space to improve. Thus, Yuan and co-workers rebuilt the PES of the ground state of the AuH_2 system by fitting 22853 *ab initio* points with neural network method (YLYC PES).[16] In their work, the dynamics calculation was also performed at the initial state ($v_0 = 0$, $j_0 = 0$) and the reaction probability, ICSs and DCSs were calculated in the collision energy range from 0.01 eV to 1.0 eV. In addition, there are also some studies on the reactions of gold ions with H_2 molecules.[17–20]

As discussed above, the reaction of Au with H_2 and its isotopic variant HD, D_2 were well studied based on the Zanchet PES. However, there are few theoretical studies of the Au + H_2/HD/D_2 reaction based on the new YLYC PES which is more accurate than the Zanchet PES at state-to-state level of theory. Thus, the aim of the present work is to perform the dynamics calculation at state-to-state level of theory and to further understand the reaction mechanism. This paper is organized as follows: the theory of TDWP and QCT methods are presented in Section 2. The state-to-state results and

†Corresponding author. E-mail: victor0536@163.com

© 2019 Chinese Physical Society and IOP Publishing Ltd

discussion are listed in Section 3, and the conclusions are described in Section 4.

2. Theoretical methods

2.1. Time-dependent wave packet method

As one of powerful computational tool of chemical reaction dynamics, the TDWP method is widely used in the atom-diatom reaction[26–33] and the reaction involving polyatomic molecules.[34,35] For the Au + H_2 reaction in the body-fixed reaction Jacobi coordinate, the Hamiltonian for a given total angular momentum J can be written as

$$\hat{H} = -\frac{\hbar^2}{2\mu_R}\frac{\partial^2}{\partial R^2} - \frac{\hbar^2}{2\mu_r}\frac{\partial^2}{\partial r^2} + \frac{(\hat{J}-\hat{j})^2}{2\mu_R R^2} + \frac{\hat{j}^2}{2\mu_r r^2} + V, \quad (1)$$

where $\hat{J}$ is the total angular momentum operator, $\hat{j}$ is the angular momentum operator of the reactant diatom molecule, μ is the reduced mass, and V is the potential energy.

Before the dynamics calculation, an initial wave packet with specific initial state should be set up. The initial wave packet consists of three parts: a Gaussian wave packet in the space-fixed frame, a ro-vibrational eigenfunction of the H_2 molecule, and a total angular momentum eigenfunction with parity of system $\varepsilon = (-1)^{j_0+l_0}$. The initial wave packet is presented as

$$\Psi^{JM\varepsilon}_{v_0 j_0 l_0}(t=0) = G(R)\,\phi_{v_0}(r)\,j_0(\theta)\,|JMj_0l_0\varepsilon\rangle. \quad (2)$$

In the calculation, the second order split operator[36] is used to propagate the initial wave packet. If the wave packet at time t is $\Psi(\hat{R},\hat{r},t)$, then after a time step Δ_t, the wave packet $\Psi(\hat{R},\hat{r},t+\Delta_t)$ can be written as

$$\Psi\left(\hat{R},\hat{r},t+\Delta_t\right) = \mathrm{e}^{-\mathrm{i}V\Delta_t/2\hbar}\mathrm{e}^{-\mathrm{i}T_j\Delta_t/2\hbar}\mathrm{e}^{-\mathrm{i}(T_r+T_R)\Delta_t/\hbar}\mathrm{e}^{-\mathrm{i}T_j\Delta_t/2\hbar} \times \mathrm{e}^{-\mathrm{i}V\Delta_t/2\hbar} \times \Psi(\hat{R},\hat{r},t), \quad (3)$$

where

$$T_j = (\hat{J}-\hat{j})^2/2\mu_R R^2 + \hat{j}^2/2\mu_r r^2,$$
$$T_R = -\hbar^2\partial^2/2\mu_R\partial R^2,$$
$$T_r = -\hbar^2\partial^2/2\mu_r\partial r^2,$$

and V is the potential energy.

The reactant coordinates based method[37,38] is used to extract the state-to-state S-matrix information. The body-fixed time-independent scattering wave function can be obtained through an orthogonal transformation matrix

$$\Phi^{J\varepsilon}_{v_v j_v l_v \leftarrow v_0 j_0 l_0}(E) = \sum_{K_v} C^{J j_v \varepsilon}_{l_v K_v}\,\Phi^{J\varepsilon}_{v_v j_v K_v \leftarrow v_0 j_0 l_0}(E). \quad (4)$$

In the space-fixed frame, using the asymptotic boundary conditions, the state-to-state scattering matrix $S^{J\varepsilon}_{v_v j_v l_v \leftarrow v_0 j_0 l_0}$ can be obtained

$$\Phi^{J\varepsilon}_{v_v j_v l_v \leftarrow v_0 j_0 l_0}\left(E;R_{v_0}\right) = -A(E)\left(\frac{2\pi\hbar^2 k_{v_v j_v}}{\mu R_v}\right)^{1/2} \times S^{J\varepsilon}_{v_v j_v l_v \leftarrow v_0 j_0 l_0}(E)\cdot\bar{H}_{l_v}(k_{v_v j_v}R_{v_0}), \quad (5)$$

where $A(E)$ is presented as

$$A(E) = \left(\frac{\mu R_\alpha}{2\pi\hbar^2 k_{v_0 j_0}}\right)^{1/2}\int \bar{H}_{l_0}\left(k_{v_0 j_0}R_\alpha\right)G(R_\alpha)\,\mathrm{d}R_\alpha, \quad (6)$$

where $\bar{H}$ is an outgoing Riccati–Hankel function.

Then, through a standard transformation, the state-to-state scattering matrix is transformed into the helicity representation

$$S^J_{v'j'K'\leftarrow vjK} = \sum_{l'l} i^{l-l'}\sqrt{\frac{2l'+1}{2J+1}}\,\langle j'K'l'0|JK'\rangle \times S^J_{v'j'K'\leftarrow vjK}\sqrt{\frac{2l+1}{2J+1}}\,\langle jKl0|JK\rangle. \quad (7)$$

Finally, the state-to-state ICS and DCS are obtained using the state-to-state S-matrix

$$\sigma_{v_v j_v \leftarrow v_0 j_0} = \sum_{K_v}\sum_{K_0}\sum_J (2J+1)\left|S^J_{v_v j_v K_v \leftarrow v_0 j_0 K_0}\right|^2, \quad (8)$$

$$\frac{\mathrm{d}\sigma_{v_v j_v \leftarrow v_0 j_0}(\vartheta,E)}{\mathrm{d}\Omega} = \frac{1}{2j_0+1} \times \sum_{K_v}\sum_{K_0}\left|\frac{1}{2\mathrm{i}k^2_{v_0 j_0}}\sum_J (2J+1)d^J_{K_v K_0}(\vartheta)S^J_{v_v j_v K_v \leftarrow v_0 j_0 K_0}\right|^2, \quad (9)$$

where $S^J_{v_v j_v K_v \leftarrow v_0 j_0 K_0}$ is the state-to-state S-matrix, $d^J_{K_v K_0}(\vartheta)$ is the reduced rotation matrix element, ϑ is the scattering angle.

2.2. Quasi-classical trajectory method

Based on the YLYC PES, standard QCT[39] calculations for the Au + H_2 ($v_0 = 0$, $j_0 = 0$) reaction were carried out in the collision energy range from 1.5 eV to 3.0 eV, with steps of 0.1 eV. The trajectories started at a distance between the incoming atom and the center of mass of the H_2 molecule of 8.0 Å, and 1000000 trajectories are sampled for each collision energy. In the calculation of trajectories, the integration step is set up as 0.02 fs to ensure the numerical stability. For the total reaction probability of total angular momentum $J = 0$, the impact parameter (b) is set as 0 and the reaction probability can be obtained by the following formula:

$$P^{J=0} = \frac{R_{\mathrm{tra}}}{N_{\mathrm{tra}}}, \quad (10)$$

where N_{tra} is the total number of trajectory, R_{tra} is the number of reaction trajectory. For the ICS and DCS calculation, b is selected randomly in the range from 0 to maximum impact parameter ($b_{\max}$) and the trajectories are terminated as the distance of the two fragments larger than 8.0 Å. The ICS and DCS can be obtained through the formulae

$$\sigma = \frac{R_{\mathrm{tra}}}{N_{\mathrm{tra}}}\cdot\pi\cdot b^2_{\max}, \quad (11)$$

$$\frac{\mathrm{d}\sigma}{\mathrm{d}\Omega} = \frac{R_{\mathrm{tra}}}{N_{\mathrm{tra}}} \cdot \frac{b_{\max}^2}{2\sin(\frac{\pi\Delta_\theta}{180})} \cdot \frac{N_\theta}{\pi}, \tag{12}$$

where Δ_θ is the angular step, N_θ is the number of grids of angular direction.

3. Result and discussion

The YLYC PES is used in the present TDWP and QCT calculations. The properties of the YLYC PES are listed in Fig. 1. As shown in the figure, the Au + H_2 reaction is an endothermic reaction and the endothermal energy is about 1.596 eV and it changes into 1.461 eV when the zero-point energy is considered. There are a shallow well, a barrier and a deep well along the minimum energy path. The depth of the wells is −0.067 eV and 0.316 eV relative to the AuH + H asymptotic channel and the barrier is about 1.296 eV higher than the energy of AuH + H asymptotic region. Compared with the Zanchet PES, the YLYS PES is more smooth and has a deeper well. For more detail one can refer to the literature.[16]

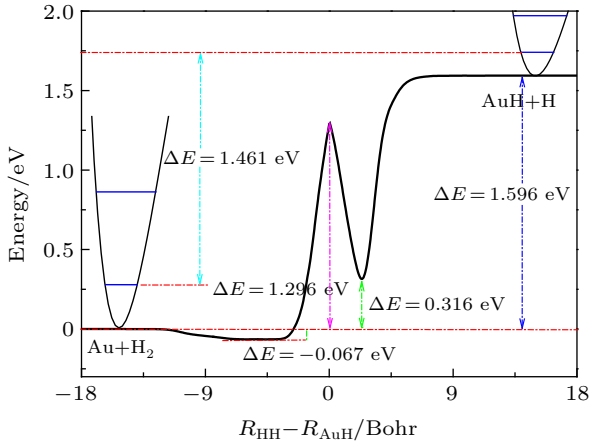


Fig. 1. The minimum energy path of the Au + H_2 reaction of the YLYC PES.

The parameters used in the TDWP calculation have large effect on the final results, thus the numerical parameters should be tested before calculation. A number of tests were performed on the total reaction probabilities of total angular momentum $J = 0$. Finally, the converged parameters were obtained and also used in the $J > 0$ calculation. The parameters are presented in Table 1.

Table 1. The numerical parameters used in the TDWP calculation (atomic unit is used unless stated otherwise).

Grid/basis range and size	$R \in [0.01, 15.0]$, $N_{\mathrm{tot}} = 255$, $N_{\mathrm{int}} = 215$, $r \in [0.0115.0]$, $N_{\mathrm{tot}} = 215$, $N_{\mathrm{asy}} = 79$, $j = 0$–99, $N_j = 49$
Initial wave packet	$\exp\left[-(R-R_{\mathrm{c}})^2/2\Delta_R^2\right]\cos(k_0 R)$, $R_{\mathrm{c}} = 12.0$, $\Delta_R = 0.18$
K-block	$\min(J+100)$
Total propagation time	30000
Time step	$\Delta_{\mathrm{t}} = 15$
Highest J value	65

The total reaction probabilities of the title reaction at the total angular momentum $J = 0$ are listed in Fig. 2 in the collision energy range from 1.4 eV to 3.0 eV along with the values calculated by the QCT method. As shown in the figure, there is a threshold about 1.461 eV, which is consistent to Fig. 1 when the zero-point energy is considered. Some resonance peaks can also be found on the TDWP reaction probabilities and the resonance peaks become mild and less apparently when the collision energy increasing. The resonance peaks can be attributed to the deep well on the reaction path, which supports a number of long life quasi-bound and bound states. With the collision energy increasing, the life time of the complex becomes shorter, thus the resonance becomes less apparently at high collision energies. From the figure we can find, the QCT values are in general good agreement with the values obtained from the TDWP method. This indicates that in the reaction of Au + H_2, the quantum effect is not so obvious and the QCT method can well describe the title reaction.

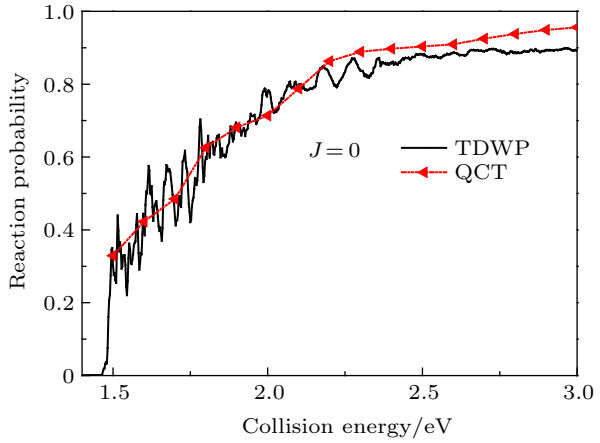


Fig. 2. The total reaction probabilities of the Au + H_2 reaction at the total angular momentum $J = 0$ along with the results of the QCT calculation.

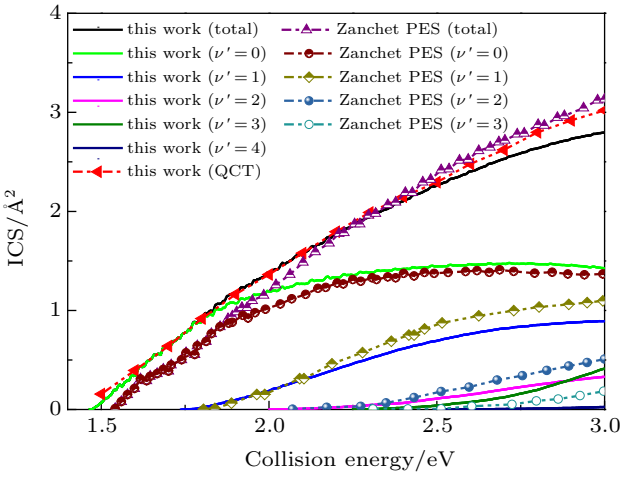


Fig. 3. The total and vibrational state-resolved ICSs of the Au + H_2 reaction along with the QCT values and the results obtained from the Zanchet PES.[14]

The total and vibrational state-resolved ICSs are presented in the Fig. 3 along with the values obtained from the

Zanchet PES[14] and the QCT calculation. As seen in the figure, the total ICS linearly increases with the collision energy increasing and the values obtained from the QCT calculation are in well agreement with the TDWP results. In addition, the values in Ref. [14] are also in general agreement with the present TDWP results. However, some discrepancies can still be found between the present TDWP values and the results obtained from the Zanchet PES. Firstly, the present values are with a relative small threshold. Secondly, although the trend of the values of Ref. [14] is similar to the present results, the values in Ref. [14] are with higher amplitude at high collision energies. Thirdly, the present values are with more vibrational states-resolved ICSs than the values in Ref. [14]. For the state-resolved ICSs, the vibrational states are gradually opened as the collision energy increases, and large difference can be found between the present values and the results in Ref. [14] when the vibrational state $v' > 0$.

The ro-vibrational state-resolved ICSs of the title reaction calculated by the TDWP method are presented in Fig. 4 at four selected collision energies. At the collision energy of 1.8 eV, there only exist two vibrational states ($v' = 0$, 1), and the peak of distribution is close to the highest rotational states. More vibrational channels are gradually opened with more rotational quantum number as the collision energy increases. It is indicated that the total available energy is effectively transferred into the internal energy. High collision energy is with more vibrational states and large rotational quantum number because more energy is available.

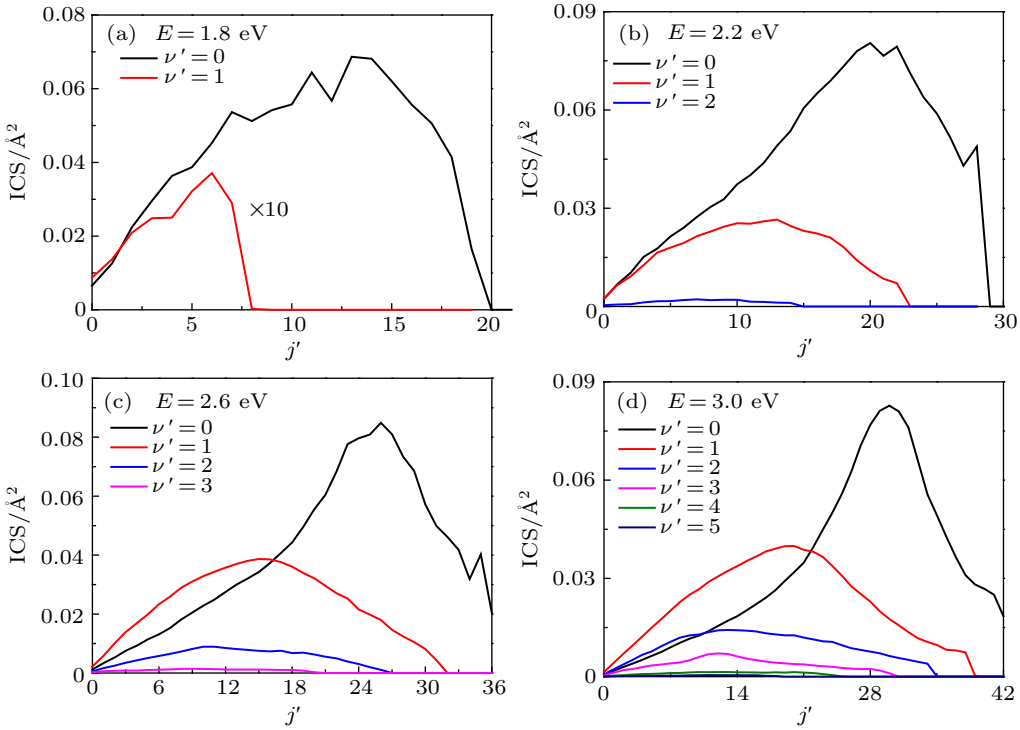


Fig. 4. The rotational distribution of AuH product at four selected collision energies.

The total DCSs of the Au + H_2 reaction at four selected collision energies 1.8 eV, 2.2 eV, 2.6 eV, and 3.0 eV are plotted in Fig. 5, as well as the QCT calculations and the values obtained in Ref. [14]. As seen in the figure, the forward and backward scattering signals are observed in the four collision energies and it tends to the forward scattering. Furthermore, the forward scattering signals become more apparent with the collision energy increasing. The QCT calculations are in good agreement with the TDWP results. This indicates that the QCT method can well describe the title reaction. The values in Ref. [14] are rather different from the present TDWP result, especially at the low collision energies. The values in Ref. [14] are almost forward-backward symmetric at the collision energies 1.8 eV and 2.2 eV, whereas the present values tend to the forward scattering. At high collision energies, the present values and the results in Ref. [14] all tend to the forward scattering. The DCS signals indicate that two reaction mechanisms can be found during the reaction. At the low collision energies, the complex-forming reaction mechanism plays a dominant role in the reaction, whereas the direct abstract reaction mechanism is dominated at high collision energies.

In order to further understand the reaction mechanism, the vibrational state-resolved DCSs of the title reaction at the collision energies of 1.8 eV, 2.2 eV, 2.6 eV, and 3.0 eV are displayed in Fig. 6. As seen in the figure, the product vibrational states increase with the collision energy increasing. As discussed above, this reflects that the collision energy is transferred into the internal energy effectively. At the collision ener-

gies of 2.2 eV, 2.6 eV, and 3.0 eV, the forward-backward symmetry scattering signals can be found on the vibrational excited states and become higher as the collision energy increasing. This reflects that the complex-forming reaction mechanism ratio becomes lower when the collision energy increases. In addition, an interesting phenomenon has been found that the side-way scattering signals become more and more apparent as the collision energy increases. This indicates that there is another reaction mechanism beyond the indirect complex-forming and direct abstract reaction mechanisms.

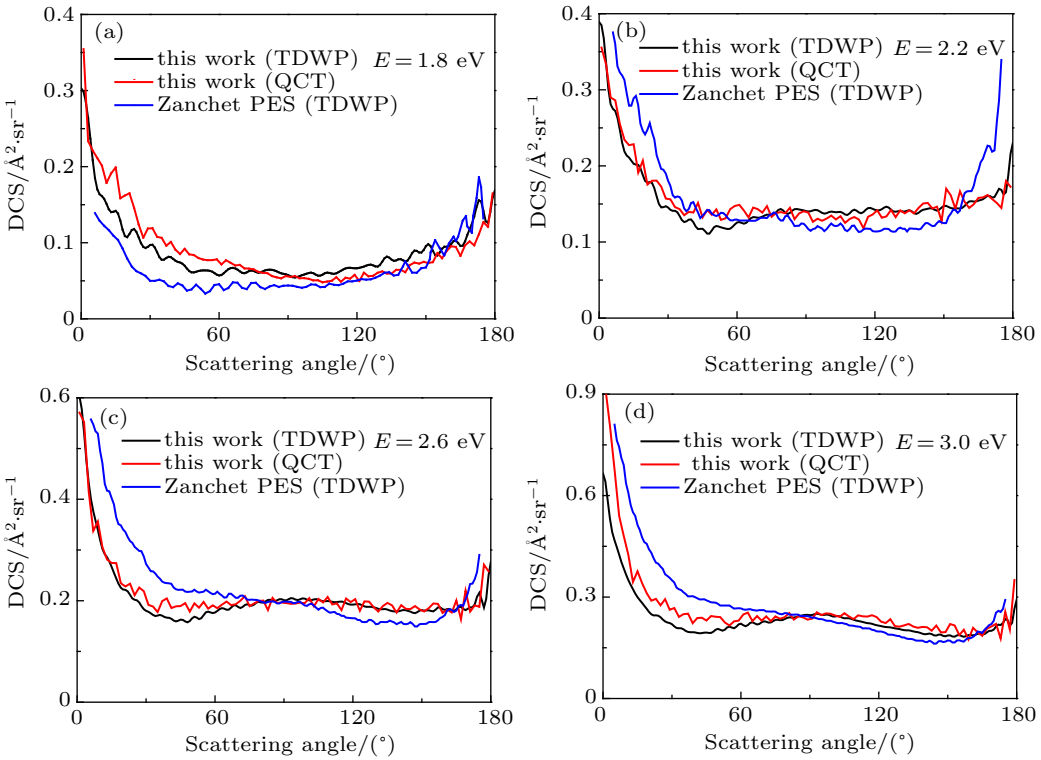


Fig. 5. The total differential cross sections of the Au + H_2 reaction at four selected collision energies along with the QCT values and the results obtained from the Zanchet PES.[14]

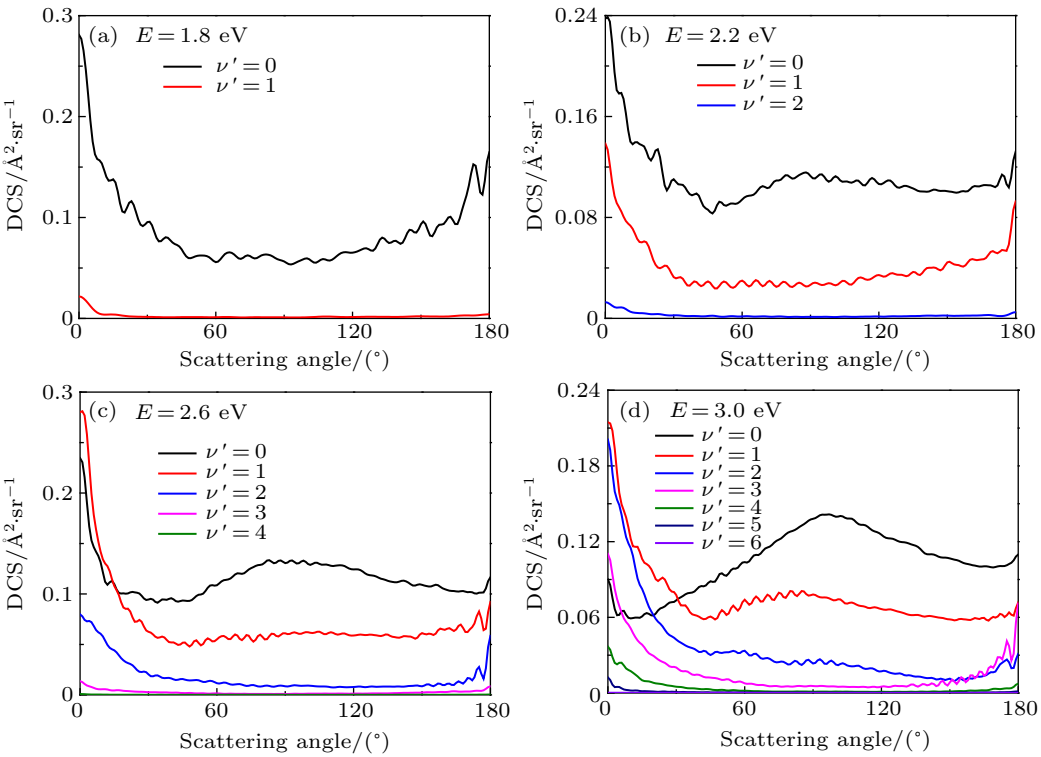


Fig. 6. The vibrational state-resolved DCSs of the Au + H_2 reaction at the collision energies of 1.8 eV, 2.2 eV, 2.6 eV, and 3.0 eV, respectively.

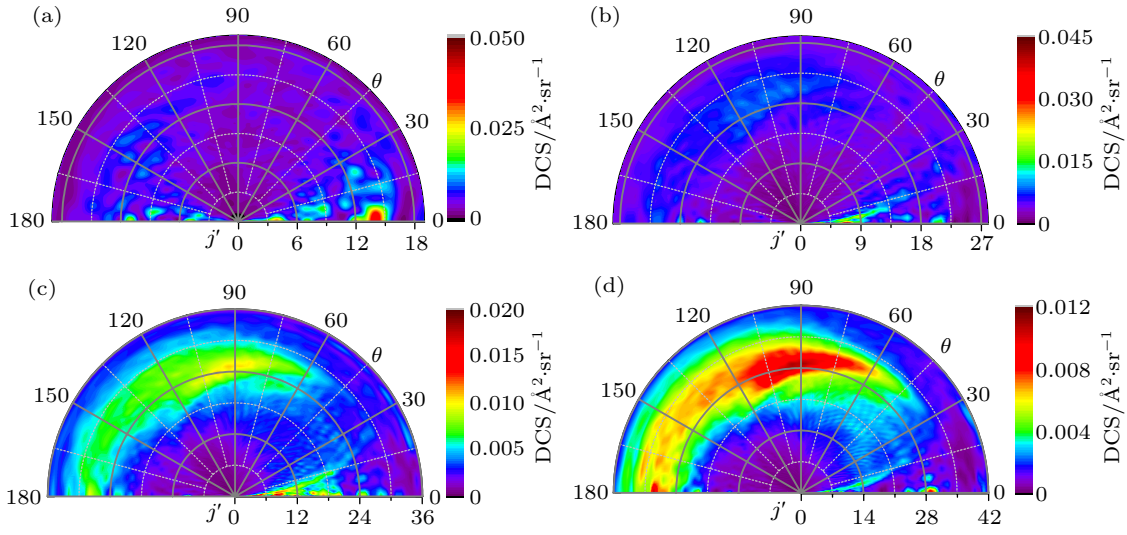


Fig. 7. The rotational state-resolved DCSs at the vibrational state $v' = 0$ of the four selected collision energies of 1.8 eV (a), 2.2 eV (b), 2.6 eV (c), and 3.0 eV (d).

In order to further understand the reaction mechanism, the rotational state-resolved DCSs of the vibrational state $v' = 0$ at the four selected collision energies. As seen in the figure, at low collision energy of 1.8 eV, it is almost forward-backward symmetry scattering. However, the side-way signals become more and more apparent when the collision energy increases and the peaks are around 90° at a relative high rotational quantum number.

4. Conclusion

The initial state $v_0 = 0$, $j_0 = 0$ dynamics calculation of the Au + H_2 reaction was carried out in the collision energy range from 0.01 eV to 1.0 eV. The TDWP method with the second order split operator and the QCT method were used in the dynamics calculations. The reaction probability, ICS, DCS, the ro-vibrational state-resolved DCS and ICS were reported and compared with previous theoretical studies. Some discrepancies can be found between previous values and the present results due to the different PESs used in the calculations. Furthermore, three reaction mechanisms were found in the dynamics calculations, the complex-forming reaction mechanism is dominated in the low collision energy region, and the abstract reaction mechanism plays a dominant at the high collision energies. In addition, the side-way scattering signals were also found when the collision energy further increases.

References

[1] Haruta M, Yamada N, Kobayashi T and Iijima S 1989 *J. Catal.* **115** 301
[2] Daniel M C and Astruc D 2004 *Chem. Rev.* **104** 293
[3] Hashmi A S K and Hutchings G J 2006 *Angew. Chem. Int. Ed.* **45** 7896
[4] Herzing A A, Kiely C J, Carley A F, Landon P and Hutchings G J 2008 *Science* **321** 1331
[5] Hughes M D, Xu Y J, Jenkins P, McMorn P, Landon P, Enache, D I, Carley A F, Attard G A, Hutchings G J, King F, Stitt E H, Johnston P, Griffin K and Kiely C J 2005 *Nature* **437** 1132
[6] Chen M S and Goodman D W 2004 *Science* **306** 252
[7] Valden M, Lai X and Goodman D W 1998 *Science* **281** 1647
[8] Yoon B, Häkkinen H, Landman U, Wörz A S, Antonietti J M, Abbet S, Judai K and Heiz U 2005 *Science* **307** 403
[9] Green I X, Tang W, Neurock M and Jr. J T Y 2011 *Science* **333** 736
[10] Balasubramanian K and Liao M Z 1988 *J. Phys. Chem.* **92** 361
[11] Andrews L, Wang X, Manceron L and Balasubramanian K 2004 *J. Phys. Chem. A* **108** 2936
[12] Guitou-Guichemerre M and Chambaud G 2005 *J. Phys. Chem.* **122** 204325
[13] Zanchet A, Roncero O, Omar S, Paniagua M and Aguado A 2010 *J. Chem. Phys.* **132** 034301
[14] Yuan J C, Cheng D H, Sun Z G and Chen M D 2014 *Mol. Phys.* **112** 2945
[15] Yuan J C, Cheng D H and Chen M D 2014 *RSC Adv.* **4** 36189
[16] Yuan M L, Li W T, Yuan J C and Chen M D 2018 *Int. J. Quantum Chem.* **118** e25493
[17] Li F, Hinton C S, Citir M, Liu F and Armentrout P B 2011 *J. Chem. Phys.* **134** 024310
[18] Dorta-Urra A, Zanchet A, Roncero O, Aguado A and Armentrou P B 2011 *J. Chem. Phys.* **135** 091102
[19] Dorta-Urra A, Zanchet A, Roncero O and Aguado A 2015 *J. Chem. Phys.* **142** 154301
[20] Lee W T, He H X and Chen M D 2017 *Int. J. Mod. Phys. B* **31** 1750039
[21] Figgen D, Rauhut G, Dolg M and Stoll H 2005 *Chem. Phys.* **311** 227
[22] Jr Dunning T H 1989 *J. Chem. Phys.* **90** 1007
[23] Aguado A and Paniagua M 1992 *J. Chem. Phys.* **96** 1265
[24] Aguado A, Suarez C and Paniagua M 1993 *J. Chem. Phys.* **98** 308
[25] Aguado A, Tablero C and Paniagua M 1998 *Comput. Phys. Commun.* **108** 259
[26] Li W T, Yuan J C, Yuan M L, Zhang Y, Yao M H and Sun Z G 2018 *Phys. Chem. Chem. Phys.* **20** 1039
[27] Li Y Q, Zhang Y J, Zhao J F, Zhao M Y and Ding Y 2015 *Chin. Phys. B* **24** 113402
[28] Xu T, Zhao J, Wang X L and Meng Q T 2019 *Chin. Phys. B* **28** 023102
[29] Zhang J, Gao S B, Wu H and Meng Q T 2015 *Chin. Phys. B* **24** 083104
[30] Wang X L, Gao F, Gao S B, Zhang L L, Song Y Z and Meng Q T 2018 *Chin. Phys. B* **27** 043104
[31] Xu T, Wu H, Zhang L L, Wang X L, Zhao J and Meng Q T 2019 *Mol. Phys.* **117** 311
[32] Zhang L L, Gao S B, Song Y Z and Meng Q T 2018 *J. Phys. B: At. Mol. Opt. Phys.* **51** 065202
[33] Gao F, Zhang L L, Zhao W L, Meng Q T and Song Y Z 2019 *J. Chem. Phys.* **150** 224304
[34] Zhao B, Sun Z G and Guo H 2016 *J. Chem. Phys.* **144** 064104
[35] Zhao B, Sun Z G and Guo H 2016 *J. Chem. Phys.* **144** 214303
[36] Feit M D, Fleck J A and Steiger A 1982 *J. Comput. Phys.* **47** 412
[37] Gómez-Carrasco S and Roncero O 2006 *J. Chem. Phys.* **125** 054102
[38] Sun Z G, Lin X, Lee S Y and Zhang D H 2009 *J. Phys. Chem. A* **113** 4145
[39] Hase W L 1998 *Classical Trajectory Simulations: Initial Conditions, A Chapter in Encyclopedia of Computational Chemistry* (New York: Wiley) Vol. **1** pp. 399, 402